Uncoupled FDA Beampattern Synthesis by Discrete Element Position and Frequency Offsets Pairing

Xiangrong Wang[#1], Qian Long[#2]
[#]School of Electronic and Information Engineering, Beihang University, Beijing, China, 100191
[1]xrwang@buaa.edu.cn, [2]qianlong0316@163.com

***Abstract*— Frequency diverse arrays (FDAs) have raised increased attention due to their ability of range-dependent beamforming and auto-scanning in angle by employing an extra frequency variation across the array elements. The range and angle of an FDA's beampattern are coupled, hence resulting in ambiguity for target detection. To overcome this problem, several methods have been proposed recently, among which pairing linearly increasing frequency offsets with a nonuniform linear array and pairing a uniform linear array with non-uniformly increasing frequency offsets are two typical employed methods. However, these methods usually assume both the element position and frequency offset can be continuously adjusted. In this paper, uncoupled FDA beampattern is synthesized by pairing two predefined sets of discrete element positions and discrete frequency offsets. As the optimum pairing of two variables requires an exhaustive search of two sets, we modify a particle swarm optimization (PSO) algorithm to solve the integer programming problem. Some numerical results are provided to verify the effectiveness of our proposed approach.**

***Keywords*— beampattern synthesis, frequency diverse array, frequency increment, non-uniform array, pairing**

I. Introduction

Frequency diverse array (FDA) was firstly proposed by Antonik *et al.* [1] in 2006 and has attracted increased attention in recent years. Unlike the conventional phased arrays, FDA is capable of producing a beampattern with controllable direction and range by shifting the carrier frequencies across the elements. Because of the characteristics of range-dependent and auto-scanning beampattern, FDA has the ability to illuminate multiple targets at different angles simultaneously [2]. Moreover, it has the potential to isolate and suppress the strong interferences at the same angle but different ranges.

The transmit beampatterns of FDAs characterize the detection performance of active radar systems and is determined by both antenna positions and shifted frequency increments. The standard uniform linear FDAs with linear frequency offset produce an S-shaped beampattern which suffers from coupling range and angle response, thus limiting their applications in target detection due to ambiguity. As a result, some methods of FDA beampattern synthesis have been proposed to achieve a range-angle decoupled beampattern [3]–[5]. Since the amplitude and spatial distribution of range-dependent pattern are controlled by the frequency shift assigned to each element and the distance between the elements of the transmit array [6], the basic idea of FDA beampatten synthesis strategies is to either adjust the frequency offsets or place the array elements in proper positions. Wassem Khan *et al.* proposed a uniformly spaced linear FDA with logarithmically increasing frequency offsets to provide a non-periodic beampattern [7]. However, this method exhibited a long tail in the response pattern, resulting in low range and angle resolution. Then a dot-shaped range-angle beampattern was achieved in [8] by optimizing the frequency increments using genetic algorithm. Similarly, [9] achieved the thumbtack-shaped FDA beampattern by applying the nonuniform logarithmic frequency offsets over a uniform linear array.

In this work, we first examine the reason why a standard FDA produces the S-shaped coupled beampattern and then propose to synthesize the uncoupled FDA beampattern by pairing two predefined sets of discrete element positions and discrete frequency offsets from the viewpoint of pragmatic implementation. As optimum subset selection is an NP-hard problem, a particle swarm optimization (PSO) algorithm is applied to solve the integer programming problem with the objective function formulated from the derived conditions.

The rest of this paper is organized as follows. Section II provides the mathematical model of FDA and derive the conditions of decoupled pattern. We then introduce the synthesis of uncoupled range-angle beampattern through proper pairing of antenna position and frequency offsets in section III. Some simulation results are provided in the Section IV and we conclude the results in Section V.

II. The Standard FDA

Consider a linear FDA composed of N identical antenna elements placed at the positions $p_n, n = 1, \ldots, N$. Each element transmits a sinusoidal waveform with a small frequency shift Δf_n from the carrier frequency f_0. Thus, the signal emitted from the n-th element of an N-element linear array is given by

$$s_n(t) = e^{2\pi f_n t} \tag{1}$$

and

$$f_n = f_0 + \Delta f_n, \quad n = 1, \cdots, N \tag{2}$$

where f_0 denotes the carrier frequency. Let us consider a standard uniform linear FDA first, $p_n = (n-1)d$ with d denoting a unit inter-element spacing and the frequency increments are also linear, $\Delta f_n = (n-1)\Delta f$ with Δf

The work by X Wang is supported by National Natural Science Foundation of China under Grant No. 61701016 and No. 61827901.

denoting the unit frequency increment. The beampattern of a standard FDA in the far field can be expressed as

$$b_p(R_0,\theta,t)=\sum_{n=0}^{N-1}\frac{w_n}{R_0}e^{j2\pi(f_n t-\frac{R_n}{\lambda_n})} \tag{3}$$

where $R_n \approx R_0 - nd\sin\theta$ denotes the distance between the n-th antenna element and the far-field target, w_n is the current excitation imposed on the nth antenna element.

To simplify Eq. (3), we assume a uniform current excitation over the array $w_0 = w_1 = \cdots = w_{N-1} = 1$. For a given time, e.g., $t = 0$, the beampattern in Eq. (3) can be rewritten into Eq. (4).

$$\begin{aligned} b_p(R_0,\theta) &\approx \sum_{n=0}^{N-1}\frac{1}{R_0}e^{-j2\pi\frac{R_n}{\lambda_n}} \\ &= \frac{1}{R_0}\sum_{n=0}^{N-1}e^{-j2\pi(f_0+n\Delta f)\frac{(R_0-nd\sin\theta)}{c}} \\ &= \frac{1}{R_0}\sum_{n=0}^{N-1}e^{j2\pi[\frac{f_0R_0}{c}-\frac{nf_0d\sin\theta}{c}+\frac{n\Delta fR_0}{c}-\frac{n^2\Delta fd\sin\theta}{c}]}, \\ &\approx \frac{1}{R_0}e^{jk_0R_0}\sum_{n=0}^{N-1}e^{-jn[k_0d\sin\theta-\Delta kR_0]}, \\ &= \frac{1}{R_0}e^{jk_0R_0}e^{-j(N-1)\varphi/2}\cdot\frac{\sin(N\varphi/2)}{\sin(\varphi/2)}, \end{aligned} \tag{4}$$

where

$$c = \text{speed of light}, \quad k_0=\frac{2\pi}{\lambda_0}=\frac{2\pi f_0}{c},$$
$$\Delta k=\frac{2\pi}{\Delta\lambda}=\frac{2\pi\Delta f}{c}, \quad \varphi=k_0d\sin\theta-\Delta kR_0.$$

Thus, the magnitude of the FDA beampattern can be expressed as,

$$|b_p(R_0,\theta)|=\frac{1}{R_0}\left|\frac{\sin(N\varphi/2)}{\sin(\varphi/2)}\right|. \tag{5}$$

The beampattern will reach a maximum when

$$\varphi=k_0d\sin\theta-\Delta kR_0=2m\pi, \quad m=0,\pm1,\cdots \tag{6}$$

Solving for range yields,

$$R_0'=\left(-\frac{c}{\Delta f}\right)m+\frac{(d/\lambda_0)c\sin\theta}{\Delta f} \tag{7}$$

We can see from Eq. (7) that, the beampattern of a standard FDA exhibits S-shaped as the range R_0' changes sinusoidally with the direction θ when grating lobes happen. This ambiguity is inherited from the standard FDA with uniformly spaced antennas and uniform frequency increments. In order to break the ambiguous beampattern of a standard FDA, either the antenna positions or frequency offsets should be adjusted properly. Ideally, the beampattern magnitude should be suppressed outside the area of interest, i.e. $b_p(r,\theta) < \epsilon,\ r \in \bar{R}, \theta \in \bar{\Theta}$, we then can achieve a thumbtack-shaped beampattern, where ϵ is a given threshold, $\bar{R}$ is the range of non-interest and $\bar{\Theta}$ is the angle of non-interest.

III. The Proposed Method

A. Mathematical Model

As continuously adjusting both antenna positions and frequency offsets is not implementable in practice, we consider to change them simultaneously by pairing two sets of discrete values in this paper. Consider a linear FDA with Q antennas, which can be placed on N potential grid points with uniform inter-element spacing of $d = \lambda_0/2$. Taking the first element as the reference, the position of the q-th element is

$$x_q = p_q d, \quad q = 1,\cdots,Q \tag{8}$$

where $p_q \in \{0,\cdots,N-1\}$. Moreover, the carrier frequency of the monotone signal emitted from the qth element is shifted from the reference frequency f_0 by an amount chosen from a set of linearly increasing frequency increments, e.g., $0, \Delta f, \cdots, (M-1)\Delta f$. The carrier frequency of the q-th element is written as,

$$f_q = f_0 + m_q\Delta f, \tag{9}$$

where m_q is an integer such that $m_q \in \{0,\cdots,M-1\}$ and M is the number of available frequency increments.

A schematic diagram of FDA element position and frequency offset pairing is shown in Fig.1. The x-axis shows the possible positions where antenna elements can be placed and the y-axis shows all the possible frequency increments. The coordinates of the q-th black square indicate both the q-th antenna position and its corresponding frequency offset from the reference carrier.

Substituting Eqs. (8) and (9) into Eq. (3), the beampattern can be rewritten as

$$\begin{aligned} b_p(R_0,\theta) &= \sum_{q=1}^{Q}e^{-j2\pi(f_0+m_q\Delta f)\cdot\frac{R_0-p_qd\sin\theta}{c}} \\ &= \sum_{q=1}^{Q}e^{-j\frac{2\pi}{c}(f_0R_0+m_q\Delta fR_0-f_0p_qd\sin\theta-m_q\Delta fp_qd\sin\theta)} \\ &\approx \sum_{q=1}^{Q}e^{-j\frac{2\pi}{c}(f_0R_0+m_q\Delta fR_0-f_0p_qd\sin\theta)} \end{aligned} \tag{10}$$

The steering vector of the transmit FDA is defined as

$$\begin{aligned} \mathbf{a}(R_0,\theta) &= [a_1(R_0,\theta), a_2(R_0,\theta), \cdots, a_Q(R_0,\theta)] \\ &= \mathbf{a}_D(\theta)\odot\mathbf{a}_R(R_0) \end{aligned} \tag{11}$$

where

$$\mathbf{a}_D(\theta)=\left[e^{jk_0p_1d\sin\theta}, e^{jk_0p_2d\sin\theta}, \cdots, e^{jk_0p_Qd\sin\theta}\right] \tag{12}$$

and

$$\mathbf{a}_R(R_0)=\left[e^{-j\Delta km_1R_0}, e^{-j\Delta km_2R_0}, \cdots, e^{-j\Delta km_QR_0}\right] \tag{13}$$

where $\odot$ denotes the Hadamard product.

In array processing, the beampattern characterizes the system response of an array beamformed in one direction to a unit amplitude target located in another direction. Assume the target is located at (R_1, θ_1), and the transmit array is beamformed towards (R_2, θ_2), the array response is

$$\rho\{(R_1,\theta_1),(R_2,\theta_2)\} = \frac{<\mathbf{a}(R_1,\theta_1),\mathbf{a}(R_2,\theta_2)>}{\|\mathbf{a}(R_1,\theta_1)\|_2\|\mathbf{a}(R_2,\theta_2)\|_2}, \quad (14)$$

where $<\cdot,\cdot>$ denotes the inner produce operation. Submitting Eqs. (12) and (13) into Eq. (14) yields,

$$\begin{aligned}
&\rho\{(R_1,\theta_1),(R_2,\theta_2)\} \quad (15)\\
&= \frac{1}{Q}[\mathbf{a}_R(R_1)\odot\mathbf{a}_D(\theta_1)]^H[\mathbf{a}_R(R_2)\odot\mathbf{a}_D(\theta_2)]\\
&= \frac{1}{Q}[\mathbf{a}_D^*(\theta_1)\odot\mathbf{a}_D(\theta_2)]^T[\mathbf{a}_R^*(R_1)\odot\mathbf{a}_R(R_2)]\\
&= \frac{1}{Q}\sum_{q=1}^{Q} e^{-jk_0p_qd(\sin\theta_1-\sin\theta_2)}e^{jk_0(R_1-R_2)}e^{j\Delta k m_q(R_1-R_2)}\\
&= \frac{1}{Q}e^{jk_0(R_1-R_2)}\sum_{q=1}^{Q} e^{-jk_0p_qd(\sin\theta_1-\sin\theta_2)}e^{j\Delta k m_q(R_1-R_2)}
\end{aligned}$$

Proceeding from Eq. (15), the amplitude of beampattern depends on the sum of Q terms, referred to as the correlation quotient $f(R_1, R_2, \theta_1, \theta_2)$. That is,

$$f(R_1,R_2,\theta_1,\theta_2) = \sum_{q=1}^{Q} e^{-jk_0p_qd(\sin\theta_1-\sin\theta_2)}e^{j\Delta k m_q(R_1-R_2)} \quad (16)$$

Then the amplitude of correlation quotient is,

$$\begin{aligned}
&|f(R_1,R_2,\theta_1,\theta_2)|^2 \quad (17)\\
&= f(R_1,R_2,\theta_1,\theta_2)\cdot f^*(R_1,R_2,\theta_1,\theta_2),\\
&= \sum_{i,q=1}^{Q}(\cos\Theta_i + j\sin\Theta_i)(\cos\Theta_q - j\sin\Theta_q),\\
&= \sum_{i,q=1}^{Q}\cos(\Theta_i-\Theta_q) + j\sin(\Theta_i-\Theta_q),
\end{aligned}$$

where

$$\Theta_q = -k_0p_qd(\sin\theta_1-\sin\theta_2) + \Delta k m_q(R_1-R_2). \quad (18)$$

As the amplitude of correlation quotient in Eq. (17) must be non-negative, i.e. $\sum_{i,q=1}^{Q}\sin(\Theta_i-\Theta_q) = 0$. Then Eq. (17) can be rewritten as

$$\begin{aligned}
|f(r_1,r_2,\theta_1,\theta_2)|^2 &= \sum_{i,q=1}^{Q}\cos(\Theta_i-\Theta_q),\\
&= Q + \sum_{i,q=1,i\neq q}^{Q}\cos(\Theta_i-\Theta_q), \quad (19)
\end{aligned}$$

where

$$\Theta_i-\Theta_q = \Delta k(m_i-m_q)(R_1-R_2) - k_0(p_i-p_q)d(\sin\theta_1-\sin\theta_2).$$

Clearly, when $R_1 = R_2$ and $\theta_1 = \theta_2$ simultaneously, Eq. (19) can achieve maximum value of N^2. The purpose of our design is to make the beampattern achieves the maximum value

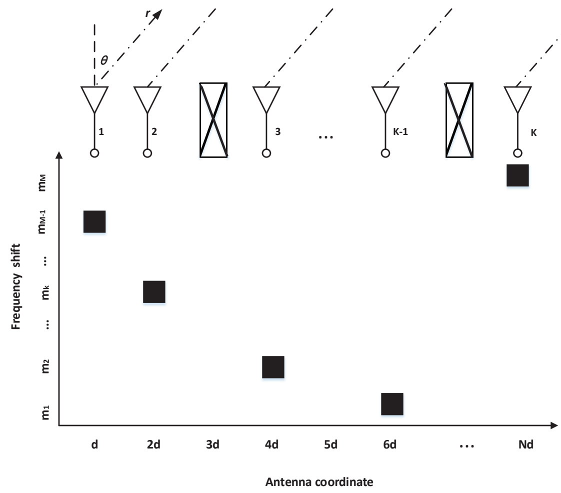

Fig. 1. Schematic diagram of FDA element position and frequency offset pairing, where the ☒ denotes the discarding antenna and the black square represents the corresponding element position and frequency shift of the selected antenna.

only once meanwhile the sidelobe is controlled under a given threshold ϵ.

Let us set

$$\xi = \Delta k(R_1-R_2), \quad \eta = -k_0d(\sin\theta_1-\sin\theta_2). \quad (20)$$

The objective function of choosing the optimum pair of antenna position and frequency offset can be expressed as

$$\sum_{i,q=1,i\neq q}^{Q}\cos\left[\xi(m_i-m_q)+\eta(p_i-p_q)\right] < \epsilon, \quad (21)$$

for the non-interested region of range $\bar{R}$ and direction $\bar{\theta}$.

B. The Modified PSO Method

Consider a transmit array with Q elements, which can be placed on N grid points and the frequency increments are selected from M candidates, the total number of pairs of element position and frequency increment is

$$K = C_N^Q \cdot A_M^Q, \quad (22)$$

where C_N^Q denotes the number of all combinations selected Q elements from N candidates and $A_M^Q = A_Q^Q C_M^Q$ denotes the product of the factorial of Q and the combination.

The computational complexity will be prohibitively high if an exhaustive search is conducted over all K possible pairs even for a moderate number. In this paper, we modify the PSO algorithm to solve the optimum pairing thanks to its excellent performance in integer programming problems. The description of PSO algorithm is summarized in Table 1.

IV. Simulation Results

To validate the effectiveness of the proposed scheme, some numerical simulations of existing FDA beamforming schemes are provided for comparison. Without loss of generality, we assume the desired beampattern is focusing on the origin $(0, 0)$.

Table 1. FDA beampattern synthesis by pairing antenna position and frequency offset using PSO

Input:	$N, M, Q, \Delta f, \epsilon, noP, G, V_{max}, w_{max}, w_{min}, c_1, c_2$
Output:	Element position, frequency offset
1	Set the dimension of searching space is equal to $N + Q$, where N-dimensional coordinates denote the element positions ('1' denotes selected, '0' denotes discard) and Q-dimensional coordinates denote frequency offsets.
2	Set population size $noP = 100$, the generations $G = 500$, $V_{max} = 10$, $w_{max} = 0.9$, $w_{min} = 0.4$ and $c_1 = c_2 = 2$.
3	Initialize the first generation of particle swarm, set $g = 1$.
4	Calculate the fitness value of particles according to the left side of Eq. (21).
5	Update the weight coefficient according to the equation $w = w_{max} - \frac{w_{max}-w_{min}}{G}$.
6	Update the global best position, optimize the particle velocity and position, then set $g = g + 1$.
7	Return to step 4 if the maximum generations G or ϵ is not attained.
8	Terminate and record the optimal pair.

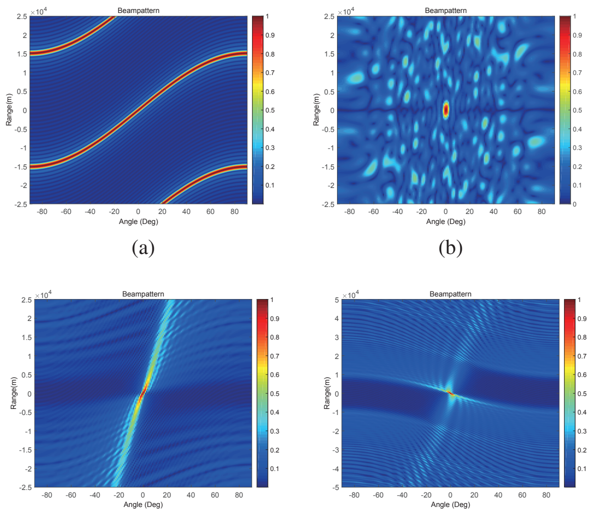

(a) (b) (c) (d)

Fig. 2. The beampattern of different frequency diverse arrays. (a) standard FDA; (b) optimize frequency increments using GA; (c) logarithmic offsets; (d) nonunioform logarithmic offsets.

The preset parameters are list in Table.2, where B denotes the generic bandwidth of signal. For proposed method, the parameters $N = 60, M = 300, Q = 49$ and the unit frequency increment $\Delta f = 1$ KHz are assumed.

In Fig.2(a), it can be seen that the standard FDA represents the S-shaped beampattern. Compare to the standard FDA, Fig.2(b) shows the synthesized dot-shaped beampattern using GA algorithm proposed on [8], which most of the energy is focus on the origin. Fig.2(c) and Fig.2(d) show the beampattern of uniform logarithmic offset and nonuniform logarithmic offset proposed in [7] and [9], respectively. It is obvious that the beampattern of nonuniform logarithmic offset is superior than the uniform one in range resolution.

The beampattern of the proposed method is presented in the Fig.3. Compare with Fig.2, the proposed method has thumbtack-shaped beampattern. It can achieve better performance in terms of range-angle resolution, peak-to-sidelobe ratio and beampattern periodicity.

Table 2. The comparison of different FDA beamforming schemes.

FDA	$f_0 = 10GHz, B = 0.3GHz, d = \lambda_0/2$	
	antennas	**array configuration**
standard FDA	30	uniform
log FDA	49	uniform
GA-optimized FDA	16	uniform
non-log FDA	49	uniform
our method	49	nonuniform

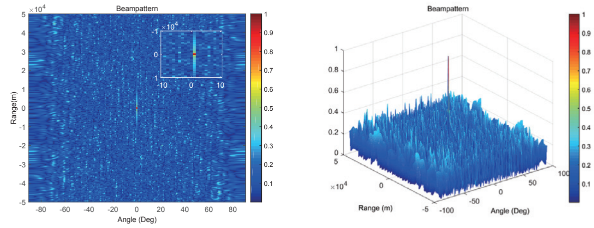

(a) (b)

Fig. 3. The beampattern of discrete element position and frequency offsets pairing. (a) 2D view, the white block is a zoom-in view of (a); (b) 3D view.

V. Conclusions

We analyzed the mathematical model of FDA beampattern synthesis and formulated an objective function to synthesize the range-angle decoupled beampattern by properly pairing the antenna positions and frequency offsets. As continuously adjusting the element position and frequency increments is not practical, we proposed to select the optimum pairing from two discrete sets in this work. The modified PSO algorithm performs well for solving the optimum pairing.

References

[1] P. Antonik, M. C. Wicks, H. D. Griffiths, and C. J. Baker, "Frequency diverse array radars," in *Radar, 2006 IEEE Conference on*. IEEE, 2006, pp. 3–pp.

[2] W.-Q. Wang, "Frequency diverse array antenna: new opportunities," *IEEE Antennas and Propagation Magazine*, vol. 57, no. 2, pp. 145–152, 2015.

[3] T. Higgins and S. D. Blunt, "Analysis of range-angle coupled beamforming with frequency-diverse chirps," in *Waveform Diversity and Design Conference, 2009 International*. IEEE, 2009, pp. 140–144.

[4] W. Khan and I. M. Qureshi, "Frequency diverse array radar with time-dependent frequency offset," *IEEE Antennas and Wireless Propagation Letters*, vol. 13, pp. 758–761, 2014.

[5] W. Li and X. Shi, "Low-sidelobe pattern synthesis in range and angle domains for frequency diverse arrays," in *2018 IEEE International Conference on Computational Electromagnetics (ICCEM)*. IEEE, 2018, pp. 1–2.

[6] P. F. Sammartino, C. J. Baker, and H. D. Griffiths, "Frequency diverse mimo techniques for radar," *IEEE Transactions on Aerospace and Electronic Systems*, vol. 49, no. 1, pp. 201–222, 2013.

[7] W. Khan, I. M. Qureshi, and S. Saeed, "Frequency diverse array radar with logarithmically increasing frequency offset," *IEEE Antennas Wireless Propag. Lett.*, vol. 14, no. 1, pp. 499–502, 2015.

[8] J. Xiong, W.-Q. Wang, H. Shao, and H. Chen, "Frequency diverse array transmit beampattern optimization with genetic algorithm," *IEEE Antennas and Wireless Propagation Letters*, vol. 16, pp. 469–472, 2017.

[9] M. Mahmood and H. Mir, "Frequency diverse array beamforming using nonuniform logarithmic frequency increments," *IEEE Antennas and Wireless Propagation Letters*, vol. 17, no. 10, pp. 1817–1821, 2018.